

T. Amieur, D. Taibi, S. Kahla, M. Bechouat, M. Sedraoui

Tilt-fractional order proportional integral derivative control for DC motor using particle swarm optimization

Introduction. Recently, the most desired goal in DC motor control is to achieve a good robustness and tracking dynamic of the set-point reference speed of the feedback control system. **Problem.** The used model should be as general as possible and consistently represent systems heterogeneous (which may contain electrical, mechanical, thermal, magnetic and so on). **Goal.** In this paper, the robust tilt-fractional order proportional integral derivative control is proposed. The objective is to optimize the controller parameters from solving the criterion integral time absolute error by particle swarm optimization. The control strategy is applied on DC motor to validate the efficiency of the proposed idea. **Methods.** The proposed control technique is applied on DC motor where its dynamic behavior is modeled by external disturbances and measurement noises. **Novelty.** The proposed control strategy, the synthesized robust tilt-fractional order proportional integral derivative speed controller is applied on the DC motor. Their performance and robustness are compared to those provided by a proportional integral derivative and fractional order proportional integral derivative controllers. **Results.** This comparison reveals superiority of the proposed robust tilt-fractional order proportional integral derivative speed controller over the remaining controllers in terms of robustness and tracking dynamic of the set-point reference speed with reduced control energy. References 21, table 1, figures 14.

Key words: DC motor, speed control, fractional order proportional integral derivative, particle swarm optimization.

Вступ. Останнім часом найбільш бажаною метою керування двигуном постійного струму є досягнення гарної надійності та динамічного відстеження заданої опорної швидкості системи керування зі зворотним зв'язком. **Проблема.** Використовувана модель має бути якомога загальнішою і несутережливо представляти різноманітні системи (які можуть містити електричні, механічні, теплові, магнітні тощо). **Мета.** У цій статті пропонується робастне управління похідною пропорційного інтеграла дробового порядку нахилу. Мета полягає в тому, щоб оптимізувати параметри контролера шляхом вирішення критерію інтегральної абсолютної тимчасової помилки шляхом оптимізації рою частинок. Стратегія управління застосовується до двигуна постійного струму для перевірки ефективності запропонованої ідеї. **Методи.** Пропонований метод управління застосовується до двигуна постійного струму, динамічна поведінка якого моделюється зовнішніми перешкодами та шумами вимірів. **Новизна.** Пропонована стратегія управління, синтезований робастний пропорційно-інтегрально-диференціальний регулятор швидкості нахилу дробового порядку застосовується до двигуна постійного струму. Їх продуктивність та надійність порівнюються з показниками, що забезпечуються контролерами пропорційної інтегральної похідної та пропорційної інтегральної похідної дробового порядку. **Результати.** Це порівняння показує перевагу запропонованого робастного пропорційно-інтегрально-диференціального регулятора швидкості нахилу дробового порядку над іншими регуляторами з погляду робастності та динамічного відстеження заданої опорної швидкості зі зменшеною енергією управління. Бібл. 21, табл. 1, рис. 14.

Ключові слова: двигун постійного струму, регулювання швидкості, пропорційна інтегральна похідна дробового порядку, оптимізація рою частинок.

Introduction. The growing interest in electric motors is justified by the need for industrial variable speed processes. This solution makes it possible to control a process or a system with minimal expenditure of energy and raw materials.

DC motor, by its very nature, has a high torque vs. speed characteristic, enabling it to deal with high resistive torques and absorb sudden rises in load effortlessly; the motor speed adapts to the load. In addition, DC motors are an ideal way of achieving the miniaturization that is so desirable to designers, since they offer a high efficiency as compared with other technologies.

The most desired goal in DC motor control is to achieve a good robustness and tracking dynamic of the set-point reference speed of the feedback control system. To achieve this goal, the used model should be as general as possible and consistently represent systems heterogeneous (which may contain electrical, mechanical, thermal, magnetic and so on), and all proposed DC motor models unavoidably incorporate uncertainties and external disturbances.

Controllers based on fractional order calculus are gaining more and more interests from the control community. This type of controllers may involve fractional operators and/or fractional systems in their structure or implementation. They have been introduced in the control applications in a continuous effort to enhance the system control quality performances and robustness.

Actually, a success among researchers is the fractional order proportional integral derivative (FOPID) [1]. In fact, since the development of the first control approach using the fractional proportional integral derivative (PID) controller, different design approaches were proposed [2-4]. On the other

hand, in recent years it is remarkable the increasing number of studies related to the application of fractional controllers in science and engineering areas [5, 6], more concretely a fractional sliding mode control [7]. In literature, fractional PID controller is frequently used to control a first order plus dead time system [8]. But, only few design methods are considered for second order plus dead time system [9]. The robust control strategies have been proposed to determine the parameters of a robust controller. The majority of them use appropriate optimization tools to solve the weighted mixed sensitivity problem such as: H_∞ control through solution of Riccati equations and linear matrix inequality approach [10, 11]. Among them, proposed a new robust tilt-PID controller based upon an automatic selection of adjustable fractional weights for permanent magnet synchronous motor drive control, the min-max optimization algorithm to solve the weighted-mixed sensitivity problem [12].

Goal. In this paper, DC motor is controlled by a proposed tilt-fractional order proportional integral derivative (T-FOPID) speed control. The parameters of the proposed controller are optimally learned by using particle swarm optimization (PSO), and the optimization performance target is chosen as the integral time absolute error (ITAE). The performance and robustness of the T-FOPID controller are compared in time domain by the FOPID and classical PID controllers. This comparison reveals the superiority of the proposed T-FOPID controller over the remaining controllers in terms of ensuring good tracking accuracy and the ability for rejecting the internal and external influences and minimization of the measurement noise.

© T. Amieur, D. Taibi, S. Kahla, M. Bechouat, M. Sedraoui

The mathematical model of DC motor. Torque of a DC motor is proportional to its armature current and current field. The winding field of a DC motor gets excited from a separate power supply, which is independent of its armature current. To achieve a linear variation of torque, one current (either field or armature) is kept constant while varying the other and it is possible in a DC motor because its current armature and field are independent of each other. Therefore, DC motors can be divided into two types depending up on how its torque is being controlled, namely armature-controlled DC motors and field-controlled DC motors.

As the discussion about the field-controlled DC motor is out of scope of this paper, we shall continue our discussion with armature-controlled DC motors.

In an armature-controlled DC motor which is shown in Fig. 1, the excitation for the winding field is kept constant and the torque is varied by varying the supply voltage connected to the armature. In some cases, a permanent magnet is used instead of winding field to produce the magnetic flux which is again independent of the armature current. Such motors are called permanent magnet DC motors [3].

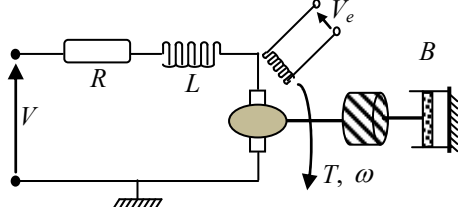


Fig. 1. Schematic diagram of the armature-controlled DC motor

A well-known linear model of DC motor for the speed control system is shown in Fig. 2.

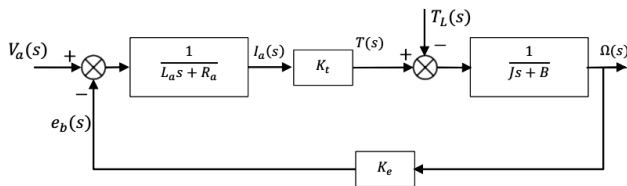


Fig. 2. Block diagram of armature-controlled DC motor

The transfer function relating the armature voltage $V_a(s)$ and angular velocity $\Omega(s)$ with $T_L(s)=0$:

$$\frac{\Omega(s)}{V_a(s)} = \frac{K_t}{L_a J s^2 + (L_a B + R_a J) s + R_a B + K_t K_e} \quad (1)$$

The transfer function relating the load torque $T_L(s)$ and angular velocity $\Omega(s)$ with $V_a(s)=0$:

$$\frac{\Omega(s)}{T_L(s)} = \frac{L_a s + R_a}{L_a J s^2 + (L_a B + R_a J) s + R_a B + K_t K_e} \quad (2)$$

The nominal values of DC motor are summarized in Table 1 [13].

Motor parameters	Value
Moment of inertia J , $\text{kg}\cdot\text{m}^2/\text{s}^2$	0.0988
Viscous friction coefficient B , $\text{N}\cdot\text{m}\cdot\text{s}/\text{rad}$	0.000587
Torque constant K_t , $\text{N}\cdot\text{m}/\text{A}$	0.67609
Armature resistance R_a , Ω	1.5
Armature inductance L , H	0.2
Voltage constant K_e , $\text{V}/(\text{rad}/\text{s})$	0.67609

Tilt-fractional order proportional integral derivative (T-FOPID). The general structure of the proposed T-FOPID controller is shown in Fig. 3.

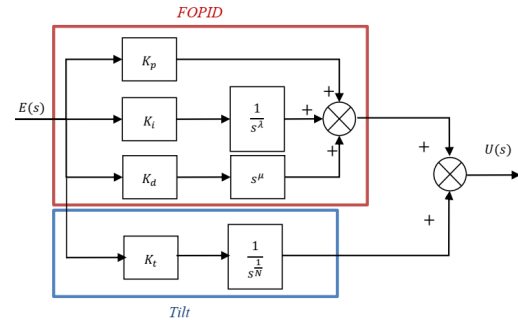


Fig. 3. Block diagram of proposed T-FOPID controller

The transfer function of the proposed T-FOPID controller is given by:

$$K(s, X) = \frac{K_t}{s^N} + \left(K_p + \frac{K_i}{s^\lambda} + K_d \cdot s^\mu \right) \quad (3)$$

The tilt component has a fractional order transfer function represented by $(s^{-1/N})$, where adjustable parameter N is preferably chosen between 2 and 3. Here, $X = (K_t, N, K_p, K_i, K_d, \lambda, \mu)^T$ is the design vector to be optimized by an adequate optimization algorithm. The search space limiting the optimal components of the proposed T-PID controller is defined by:

$$\begin{cases} K_{t_{\min}} \leq K_t \leq K_{t_{\max}}; \\ 2 \leq N \leq 3; \\ K_{p_{\min}} \leq K_p \leq K_{p_{\max}}; \\ K_{i_{\min}} \leq K_i \leq K_{i_{\max}}; \\ K_{d_{\min}} \leq K_d \leq K_{d_{\max}}; \\ 0 < \lambda < 1; \\ 0 < \mu < 1. \end{cases} \quad (4)$$

Tuning of T-FOPID by PSO algorithm. Many intelligence algorithms are proposed for tuning the T-FOPID parameters. Tuning T-FOPID parameters by the optimal algorithms such as the genetic algorithm and PSO algorithm. However, it is slow to search the best solution [14, 15].

The PSO concept consists of changing the velocity (or acceleration) of each particle toward its p_{best} and the g_{best} position at each time step. Each particle tries to modify its current position and velocity according to the distance between its current position and p_{best} , and the distance between its current position and g_{best} as shown in the following. At each step n , by using the individual best position, p_{best} , and global best position, g_{best} , a new velocity for the i^{th} particle is updated by [16]:

$$V_i(n) = wV_i(n-1) + c_1 r_1 (p_{best_i} - p_i(n-1)) + c_2 r_2 (g_{best_i} - p_i(n-1)) \quad (5)$$

where w is the constriction factor; p_i is the position vector; r_1 and r_2 are the random numbers between $[0; 1]$; c_1 and c_2 are the positive constant learning rates, called self-confidence and swarm confidence respectively.

Each of the three terms of the velocity update equation has different roles in the PSO algorithm [17].

The first term $wV_i(n)$ is the inertia component, which is responsible for keeping the particle moving in the same direction as it was originally heading. The value of the inertial coefficient w is typically between 0.8 and 1.2, which can either dampen the particle's inertia or accelerate the

particle in its original direction. Generally, lower values of the inertial coefficient speed up the convergence of the swarm to optima, and higher values of the inertial coefficient encourage exploration of the entire search space [18].

The second term $c_1 r_1 (p_{best} - p_i(n-1))$, called the cognitive component, which acts as the particle's memory, causing it to tend to return to the regions of the search space in which it has experienced high individual fitness. The cognitive coefficient c_1 is usually close to 2, and affects the size of the step that the particle takes toward its individual best candidate solution p_{best} .

The third term $c_2 r_2 (g_{best} - p_i(n-1))$, called the social component, causes the particle to move to the best region that the swarm has found so far. The social coefficient c_2 is typically close to 2, and represents the size of the step that the particle takes toward the global best candidate solution g_{best} the swarm has found up until that point.

The random values r_1 in the cognitive component and r_2 in the social component which causes these components to have a stochastic influence on the velocity update. This stochastic nature causes each particle to move in a semi-random manner heavily influenced in the directions of the individual best solution of the particle and global best solution of the swarm.

In order to keep the particles from moving too far beyond the search space, we use a technique called velocity clamping to limit the maximum velocity of each particle. For a search space bounded by the range $[p_{min}, p_{max}]$, velocity clamping limits the velocity to the range $[V_{min}, V_{max}]$, where $V_{max} = k(p_{max} - p_{min})/2$. The value represents a user-supplied velocity clamping factor, $0.1 \leq k \leq 1$.

Based on the updated velocity, each particle changes its position as follows [19]:

$$p_i(n) = p_i(n-1) + V_i(n). \quad (6)$$

The position is confined within the range of $[p_{min}, p_{max}]$. If the position violates these limits, it is forced to its proper values. Changing position by this way enables the i^{th} particle to search around its local best position, p_{best} , and global best position, g_{best}

$$p_i = \begin{cases} p_{min} & \text{if } p_i < p_{min}; \\ p_i & \text{if } p_{min} < p_i < p_{max}; \\ p_{max} & \text{if } p_i > p_{max}; \end{cases} \quad (7)$$

The PSO is an algorithm with population. It starts with a random initialization of the swarm in the space of research. With each iteration of the algorithm, each particle is moved according to the equations of motion which are given by (5), (6).

Objective function. As already mentioned, the fitness function to be minimized is the ITAE performance criterion [20, 21]. The integral of the absolute magnitude of error (ITAE) criterion is defined as

$$ITAE = \int_0^T |e(t)| dt. \quad (8)$$

The ITAE performance criterion index has the advantages of producing smaller overshoots and oscillations than the IAE (integral of the absolute error) or the ISE (integral square error) performance indices. In addition, it is the most sensitive of the three, i.e., it has the best selectivity. The ITSE (integral time-square error)

index is somewhat less sensitive and is not comfortable computationally. Since it is not practicable to integrate up to infinity, the convention is to choose a value of T sufficiently large so that $e(t)$ for $t > T$ is negligible.

Tuning parameters of T-FOPID by PSO algorithm.

Optimization by PSO consists of designing the optimization goal, i.e., the fitness function and then encoding the parameters to be searched. The PSO algorithm runs until the stop condition is satisfied. The best particle's position gives the optimized parameters.

The parameters of the T-FOPID controller (Fig. 4) to be optimized has seven unknown parameters to be tuned $X = (K_t, N, K_p, K_i, K_d, \lambda, \mu)^T$. Hence the present problem of controller tuning can be solved by an application of the PSO algorithm for optimization on a seven-dimensional solution space, each particle has a seven-dimensional position and velocity vector.

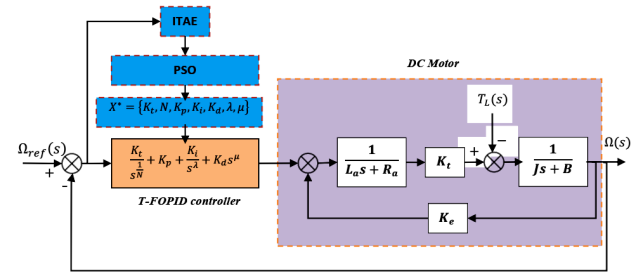


Fig. 4. Feedback T-FOPID control of DC motor

The optimization process based on the PSO is summarized by the flowchart, depicted in Fig. 5.

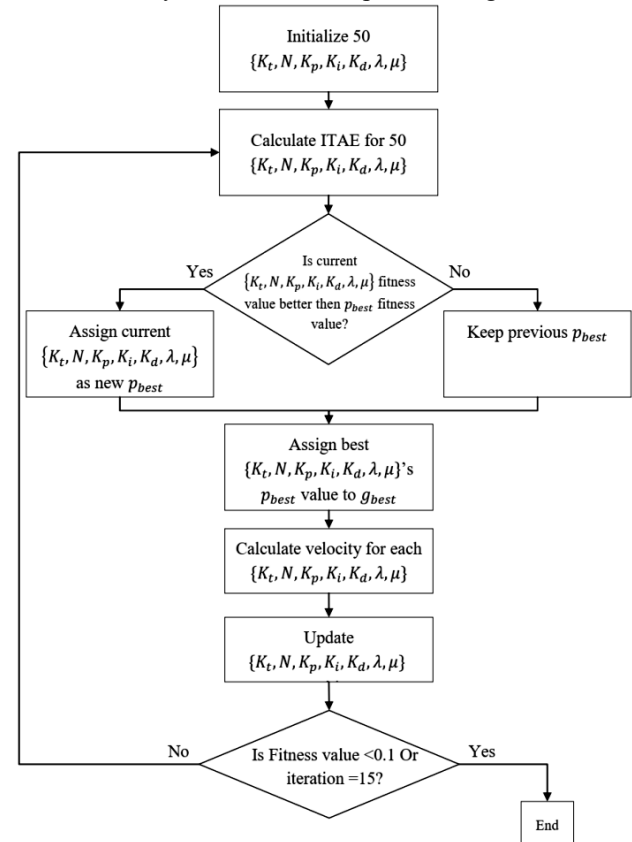


Fig. 5. The flowchart providing the robust T-FOPID speed controller tuning by PSO algorithm

Simulation results and discussion. The nominal values of DC motor are summarized in Table 1, the nominal voltage

$V_a = 120$ V. The transfer function relating the armature voltage $V_a(s)$ and angular velocity $\Omega(s)$ with $T_L(s) = 0$:

$$\frac{\Omega(s)}{V_a(s)} = \frac{0.67609}{0.01976 \cdot s^2 + 0.14832 \cdot s + 0.45798}$$

The transfer function relating the load torque $T_L(s)$ and angular velocity $\Omega(s)$ with $V_a(s) = 0$:

$$\frac{\Omega(s)}{T_L(s)} = \frac{0.2 \cdot s + 1.5}{0.01976 \cdot s^2 + 0.14832 \cdot s + 0.45798}$$

The corresponding optimization problem contains seven unknown variables. It is expressed as follows:

$$X^* \subset X = \begin{cases} 0 \leq K_t \leq 3; \\ 2 \leq N \leq 3; \\ 0 \leq K_p \leq 50; \\ 0 \leq K_i \leq 50; \\ 0 \leq K_d \leq 5; \\ 0 < \lambda < 1; \\ 0 < \mu < 1. \end{cases}$$

This problem is solved by the PSO, in which the following tuning parameters are used (Fig. 6):

- SwarmSize = 50;
- OFun = @FFtfopidfunction;
- MaxIter = 15;
- MinFit = 0.1.

The provided optimal solution X^* by the PSO allows determining the following T-FOPID, FOPID and PID controllers [15]:

$$K_{T-FOPID}(s) = \frac{0.501}{s^{1/3}} + 16.6384 + \frac{30}{s^{0.8144}} + 2.2729 \cdot s^{0.9049};$$

$$K_{FOPID}(s) = 12.1348 + \frac{50}{s^{0.985}} + 2.4856 \cdot s^{0.979};$$

$$K_{PID}(s) = 15.3326 + \frac{36.8206}{s} + 2.029 \cdot \left(\frac{180.2349}{1 + 180.2349 \cdot \left(\frac{1}{s} \right)} \right)$$

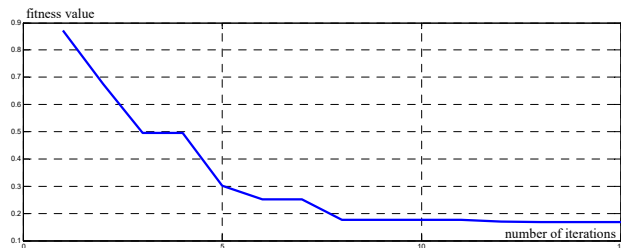


Fig. 6. The best provided minimization using the PSO of the fitness value

The above mentioned three controllers are connected with the linear nominal DC model and the obtained feedback control system is then excited by the three exogenous inputs: mechanical speed reference, disturbance and sensor noise signals. The load torque input $T_L = 20$ N·m, applied at the starting time $t = 4$ s. The random signal of zero mean and Gaussian distribution with a variance equal to 10^{-3} with the star-time $t = 7$ s. Therefore, Fig. 7, 11, 12, 14 compare the mechanical speeds provided by the three PID, FOPID and T-FOPID

speed controllers. Otherwise, where their control signals are compared in Fig. 14.

Tracking echelon signal reference speed. The nominal reference speed of this motor is 157 rad/s (120 V is the supply voltage).

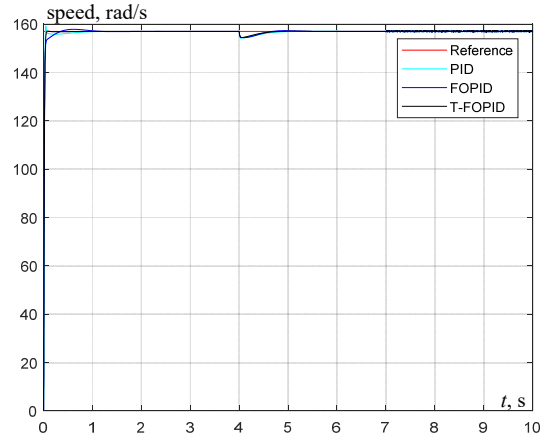


Fig. 7. The given speed with torque load and measurement noise presence

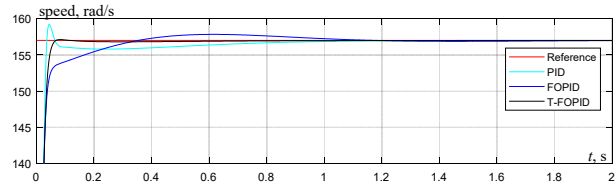


Fig. 8. Zoom of the given speed parts of transient-state

Torque load rejection. The presence of the load torque input $T_L = 20$ N·m, which is applied at the starting time $t = 4$ s. From the Fig. 7, we conclude that the T-FOPID controller allows tracking the reference speed with high accuracy. Figure 8, the zoom parts given speed of transient-state and Fig. 9, the zoom parts given speed of the presence load torque input $T_L = 20$ N·m, applied at the starting time $t = 4$ s. In Fig. 10, the zoom parts give speed of the presence measurement noise random signal of zero mean and Gaussian distribution with a variance equal to 10^{-3} with the star-time $t = 7$ s.

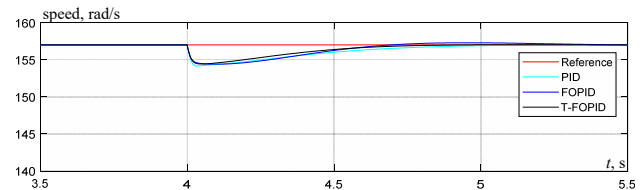


Fig. 9. Zoom of the given speed parts of torque load

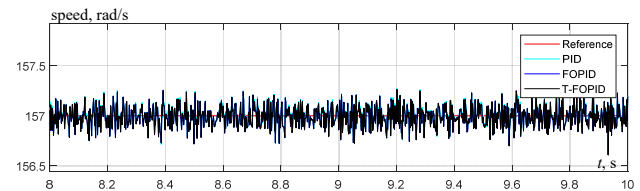


Fig. 10. Zoom of the given speed parts of measurement noise

Tracking rectangular signal reference speed. Used to excite the feedback control system. The input is assumed by:

$$\omega_{ref} = \begin{cases} 157 \text{ rad/s} & 0 \leq t \leq 2 \text{ s and } 6 \text{ s} < t \leq 10 \text{ s;} \\ -157 \text{ rad/s} & 2 \text{ s} \leq t \leq 6 \text{ s.} \end{cases}$$

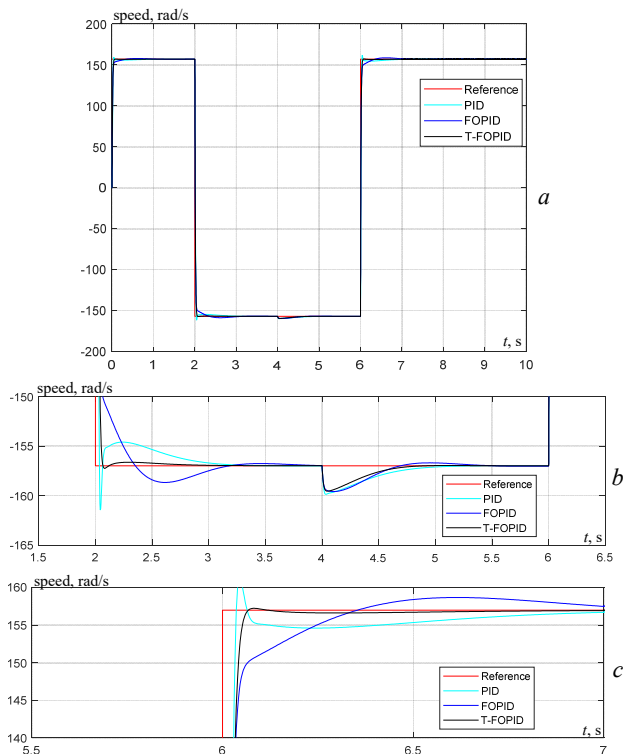


Fig. 11. *a* – the given speed for reference speed rectangular signal by the three controllers *PID*, *FOPID* and *T-FOPID*; *b*, *c* – the zoom parts

Tracking sinusoidal signal reference speed. The reference speed input is assumed to be a sinusoidal signal based sample type. It is given with the amplitude $A = 157$, where 100 samples per period $T = 3.14$ s.

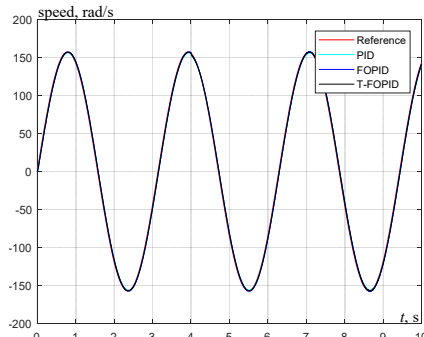


Fig. 12. Mechanical speeds given by the three controllers *PID*, *FOPID* and *T-FOPID*

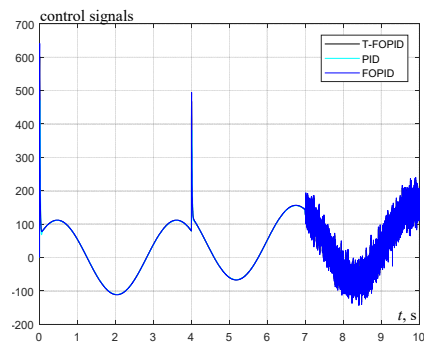


Fig. 13. Control signals by the three *PID*, *FOPID* and *T-FOPID* speed controllers

Therefore, the output signals given with *T-FOPID*, *FOPID* and *PID* controllers are compared in Fig. 12,

where in their control signals are compared in Fig. 13 with reference speed input is a sinusoidal signal.

Tracking triangular signal reference speed. The second reference speed input is assumed to be a triangular signal with the amplitude $A = 157$ and the period $T = 2$ s.

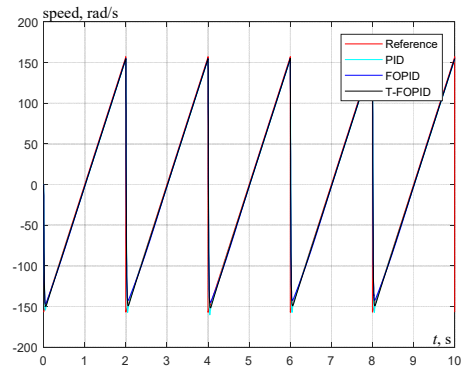


Fig. 14. Mechanical speeds given by the three controllers *PID*, *FOPID* and *T-FOPID*

Despite changing the speed to several forms (rectangular signal Fig. 11, sinusoidal signal Fig. 12 and triangular signal Fig. 14), we note that the *T-FOPID* controller tracks it with high accuracy.

Conclusions. In this paper we have proposed the new robust tilt-fractional order proportional integral derivative controller, for the optimization of parameters in this controller we used the particle swarm optimization algorithm. It is a very simple and efficient algorithm which gave optimal parameters of proposed controller, based on the integral time absolute error criterion. The speed of a DC motor in a closed loop with tilt-fractional order proportional integral derivative controller. First, we subjected the dc motor to different speeds (constant signal, rectangular signal, sinusoidal signal and triangular signal), we noticed the ability of the proposed controller to change the dc motor speed to follow these speeds with high accuracy in a short time. Secondly, we studied the efficiency of the proposed controller in rejecting the external influences (torque load) and minimization of the measurement noise. Finally, we compared the performance of the proportional integral derivative and fractional order proportional integral derivative controllers to confirm the superiority and efficiency of the tilt-fractional order proportional integral derivative controller in tracking accuracy and the ability to reject the internal and external influences. Based on these results, it can be said that the proposed controller is very effective and reliable in controlling the speed of the *DC* motor.

Conflict of interest. The authors declare that they have no conflicts of interest.

REFERENCES

- Podlubny I. Fractional-order systems and $PI^\lambda D^\mu$ -controllers. *IEEE Transactions on Automatic Control*, 1999, vol. 44, no. 1, pp. 208-214. doi: <https://doi.org/10.1109/9.739144>.
- Monje C.A., Vinagre B.M., Feliu V., Chen Y. Tuning and auto-tuning of fractional order controllers for industry applications. *Control Engineering Practice*, 2008, vol. 16, no. 7, pp. 798-812. doi: <https://doi.org/10.1016/j.conengprac.2007.08.006>.
- Amieur T., Sedraoui M., Amieur O. Design of Robust Fractional-Order PID Controller for DC Motor Using the Adjustable Performance Weights in the Weighted-Mixed Sensitivity Problem. *IAES International Journal of Robotics and*

- Automation (IJRA)*, 2018, vol. 7, no. 2, pp. 108-118. doi: <https://doi.org/10.11591/ijra.v7i2.pp108-118>.
4. Regad M., Helaimi M., Taleb R., Gabbar H., Othman A. Optimal frequency control in microgrid system using fractional order PID controller using krill herd algorithm. *Electrical Engineering & Electromechanics*, 2020, no. 2, pp. 68-74. doi: <https://doi.org/10.20998/2074-272X.2020.2.11>.
 5. Barbosa R.S., Tenreiro Machado J.A., Jesus I.S. Effect of fractional orders in the velocity control of a servo system. *Computers & Mathematics with Applications*, 2010, vol. 59, no. 5, pp. 1679-1686. doi: <https://doi.org/10.1016/j.camwa.2009.08.009>.
 6. Tavakoli-Kakhki M., Haeri M. Fractional order model reduction approach based on retention of the dominant dynamics: Application in IMC based tuning of FOPI and FOPID controllers. *ISA Transactions*, 2011, vol. 50, no. 3, pp. 432-442. doi: <https://doi.org/10.1016/j.isatra.2011.02.002>.
 7. Ardjal A., Mansouri R., Bettayeb M. Fractional sliding mode control of wind turbine for maximum power point tracking. *Transactions of the Institute of Measurement and Control*, 2019, vol. 41, no. 2, pp. 447-457. doi: <https://doi.org/10.1177/0142331218764569>.
 8. Li M., Zhou P., Zhao Z., Zhang J. Two-degree-of-freedom fractional order-PID controllers design for fractional order processes with dead-time. *ISA Transactions*, 2016, vol. 61, pp. 147-154. doi: <https://doi.org/10.1016/j.isatra.2015.12.007>.
 9. Chen K., Tang R., Li C. Phase-constrained fractional order PI^λ controller for second-order-plus dead time systems. *Transactions of the Institute of Measurement and Control*, 2017, vol. 39, no. 8, pp. 1225-1235. doi: <https://doi.org/10.1177/0142331216634427>.
 10. Aidoud M., Sedraoui M., Lachouri A., Boualleg A. A robustification of the two degree-of-freedom controller based upon multivariable generalized predictive control law and robust H_∞ control for a doubly-fed induction generator. *Transactions of the Institute of Measurement and Control*, 2018, vol. 40, no. 3, pp. 1005-1017. doi: <https://doi.org/10.1177/0142331216673425>.
 11. Patra S., Sen S., Ray G. A linear matrix inequality approach to parametric H_∞ loop shaping control. *Journal of the Franklin Institute*, 2011, vol. 348, no. 8, pp. 1832-1846. doi: <https://doi.org/10.1016/j.jfranklin.2011.05.006>.
 12. Amieur T., Bechouat M., Sedraoui M., Kahla S., Guessoum H. A new robust tilt-PID controller based upon an automatic selection of adjustable fractional weights for permanent magnet synchronous motor drive control. *Electrical Engineering*, 2021, vol. 103, no. 3, pp. 1881-1898. doi: <https://doi.org/10.1007/s00202-020-01192-3>.
 13. Aashoor F.A.O., Robinson F.V.P. Maximum power point tracking of PV water pumping system using artificial neural based control. *3rd Renewable Power Generation Conference (RPG 2014)*, Naples, 2014, pp. 1-6, doi: <https://doi.org/10.1049/cp.2014.0923>.
 14. Aghababa M.P. Optimal design of fractional-order PID controller for five bar linkage robot using a new particle swarm optimization algorithm. *Soft Computing*, 2016, vol. 20, no. 10, pp. 4055-4067. doi: <https://doi.org/10.1007/s00500-015-1741-2>.
 15. Hekimoglu B. Optimal Tuning of Fractional Order PID Controller for DC Motor Speed Control via Chaotic Atom Search Optimization Algorithm. *IEEE Access*, 2019, vol. 7, pp. 38100-38114. doi: <https://doi.org/10.1109/ACCESS.2019.2905961>.
 16. Anwar N., Hanif A., Ali M.U., Zafar A. Chaotic-based particle swarm optimization algorithm for optimal PID tuning in automatic voltage regulator systems. *Electrical Engineering & Electromechanics*, 2021, no. 1, pp. 50-59. doi: <https://doi.org/10.20998/2074-272X.2021.1.08>.
 17. Bouraghda S., Sebaa K., Bechouat M., Sedraoui M. An improved sliding mode control for reduction of harmonic currents in grid system connected with a wind turbine equipped by a doubly-fed induction generator. *Electrical Engineering & Electromechanics*, 2022, no. 2, pp. 47-55. doi: <https://doi.org/10.20998/2074-272X.2022.2.08>.
 18. Marini F., Walczak B. Particle swarm optimization (PSO). A tutorial. *Chemometrics and Intelligent Laboratory Systems*, 2015, vol. 149, pp. 153-165. doi: <https://doi.org/10.1016/j.chemolab.2015.08.020>.
 19. Kao C.-C., Chuang C.-W., Fung R.-F. The self-tuning PID control in a slider-crank mechanism system by applying particle swarm optimization approach. *Mechatronics*, 2006, vol. 16, no. 8, pp. 513-522. doi: <https://doi.org/10.1016/j.mechatronics.2006.03.007>.
 20. Kumar Sahu R., Panda S., Biswal A., Chandra Sekhar G.T. Design and analysis of tilt integral derivative controller with filter for load frequency control of multi-area interconnected power systems. *ISA Transactions*, 2016, vol. 61, pp. 251-264. doi: <https://doi.org/10.1016/j.isatra.2015.12.001>.
 21. Barisal A.K. Comparative performance analysis of teaching learning based optimization for automatic load frequency control of multi-source power systems. *International Journal of Electrical Power & Energy Systems*, 2015, vol. 66, pp. 67-77. doi: <https://doi.org/10.1016/j.ijepes.2014.10.019>.

Received 13.10.2022
Accepted 08.12.2022
Published 07.03.2023

Toufik Amieur^{1,2}, Associate Professor,
Djamel Taïbi³, PhD, Assistant Professor,
Sami Kahla⁴, Associate Professor,
Mohcene Bechouat^{2,5}, PhD, Associate Professor,
Moussa Sedraoui², Professor,
¹ Department of Electrical Engineering,
Echahid Cheikh Larbi Tebessi University-Tebessa, Algeria
² The Telecommunications Laboratory (LT),
University 8 May 1945 Guelma, Algeria,
e-mail: amieur.toufik@univ-tebessa.dz (Corresponding Author);
sedraoui.moussa@univ-guelma.dz
³ Department of Electrical Engineering,
Kasdi Merbah University-Ouargla, Algeria,
e-mail: taïbi.djamel@yahoo.fr
⁴ A Research Center in Industrial Technologies (CRTI), Algeria,
e-mail: samikahla40@yahoo.com
⁵ Automatic and Electromechanic Department,
University of Ghardaia, Algeria,
e-mail: mohcene.oui@gmail.com

How to cite this article:

Amieur T., Taïbi D., Kahla S., Bechouat M., Sedraoui M. Tilt-fractional order proportional integral derivative control for DC motor using particle swarm optimization. *Electrical Engineering & Electromechanics*, 2023, no. 2, pp. 14-19. doi: <https://doi.org/10.20998/2074-272X.2023.2.03>